PROCEEDINGS OF SCIENCE

Recent results on baryon spectroscopy at ELSA and MAMI

F. Afzal for the CBELSA/TAPS and A2 collaborations[a,*]

[a] *Ruhr University Bochum,*
Universitätsstraße 150, 44801 Bochum, Germany

E-mail: FarahNoreen.Afzal@ruhr-uni-bochum.de

Baryon spectroscopy gives insights into the dynamics between the constituents of baryons and study quantum chromodynamics (QCD) in the non-perturbative regime. Quark models and Lattice QCD calculations predict a large number of baryons, but only a fraction of them have been found experimentally. The baryon spectra can be probed with a real photon beam by studying various different photoproduction reactions. Partial-wave analyses need to be performed to extract the baryon resonance parameters from the experimental data. For an unambiguous solution, several single and carefully chosen double polarization observables are needed in addition to the unpolarized cross section.

Worldwide, various experimental facilities have dedicated programs to measure these polarization observables in different photoproduction reactions using polarized photon beams and polarized targets. Two of the leading experimental facilities are located in Germany, the CBELSA/TAPS experiment at the accelerator facility ELSA in Bonn and the Crystal Ball experiment at the accelerator facility MAMI in Mainz. Both experiments are excellent at measuring neutral mesons in the final states, using electromagnetic calorimeters covering almost the full angular range, while exploring complementary beam energy regions. This contribution will give an overview about recent results in non-strange baryon spectroscopy at ELSA and MAMI.

The XVIth Quark Confinement and the Hadron Spectrum Conference (QCHSC24)
19-24 August, 2024
Cairns Convention Centre, Cairns, Queensland, Australia

*Speaker

 ISSN 1824-8039 . Published by SISSA Medialab.

PoS(QCHSC24)080

1. Introduction

One of the most challenging tasks of hadron physics is to map out the nucleon excitation spectrum and understand the underlying effective degrees of freedom. The nucleon excitation spectrum can be calculated using different approaches. There are e.g. several quark models that treat baryons as bound states of three massive constituent quarks and use a confinement potential and residual quark-quark interactions [1]. In addition, lattice QCD calculations have also been used to calculate the baryon spectra [2]. Both approaches predict a large number of baryons. However, only a fraction of them have been found experimentally so far.

There has been a worldwide effort to probe the excitation spectrum with different production mechanisms and search for the *missing resonances*. The experimental search for light-quark baryons is quite challenging since the spectrum of N^* and Δ^* is expected to be dense in the mass range below 2.5 GeV. In addition, the resonances are broad due to the strong interaction, and they can overlap and interfere. The CBELSA/TAPS experiment at the accelerator ELSA and the Crystal Ball experiment at the accelerator MAMI use a real photon beam to investigate the nucleon excitation spectrum. To disentangle all the contributing baryon resonances and get an unambiguous solution, it is important to measure in addition to the unpolarized cross section also single and double polarization observables. This can be achieved by using a polarized photon beam, a polarized target or by measuring the recoil nucleon polarization. Table 1 shows the polarization observables that be accessed in case of the photoproduction of a single pseudo-scalar meson.

photon		**target**			**recoil nucleon**			**target and recoil**			
		x	y	z	-	-	-	x	z	x	z
		-	-	-	x'	y'	z'	x'	x'	z'	z'
-	σ_0	-	T	-	-	P	-	$T_{x'}$	$L_{x'}$	$T_{z'}$	$L_{z'}$
linear	Σ	H	P	G	$O_{x'}$	T	$O_{z'}$	$L_{z'}$	$T_{z'}$	$L_{x'}$	$T_{x'}$
circular		F	-	E	$C_{x'}$	-	$C_{z'}$	-	-	-	-

Table 1: Accessible polarization observables in single pseudoscalar photoproduction. [3]

2. The CBELSA/TAPS and the Crystal Ball experiments

The CBELSA/TAPS experiment is located at the electron stretcher accelerator ELSA [4] in Bonn, Germany. The electrons are accelerated up to an energy of 3.2 GeV. The Crystal Ball experiment is located at the electron accelerator MAMI [5] in Mainz, Germany. Here, the maximal available electron beam energy is 1.6 GeV. Both experiments have several aspects in common: Both use bremsstrahlung to produce a real photon beam. The photon beam can be either linearly or circularly polarized using either a diamond or an amorphous radiator and choosing unpolarized or longitudinally polarized electrons. In addition, polarized frozen-spin targets are available for measurements. Both detector setups consist mainly of two electromagnetic calorimeters (Crystal Barrel and MiniTAPS, and Crystal Ball and TAPS, respectively) that cover almost the full solid angle. Charged particles are detected with a three-layer scintillating fiber detector surrounding the target and plastic scintillators mounted in front of the first three rings of the Crystal Barrel calorimeter and the MiniTAPS detector (CBELSA/TAPS experiment), or with the scintillation

detectors surrounding the target (PID) and in front of the TAPS calorimeter, as well as two Multi-Wire Proportional Chambers (Crystal Ball experiment). More details about the respective detector setups are given in [6, 7]. An overview of both experiments is shown in Fig. 1. The experiments are

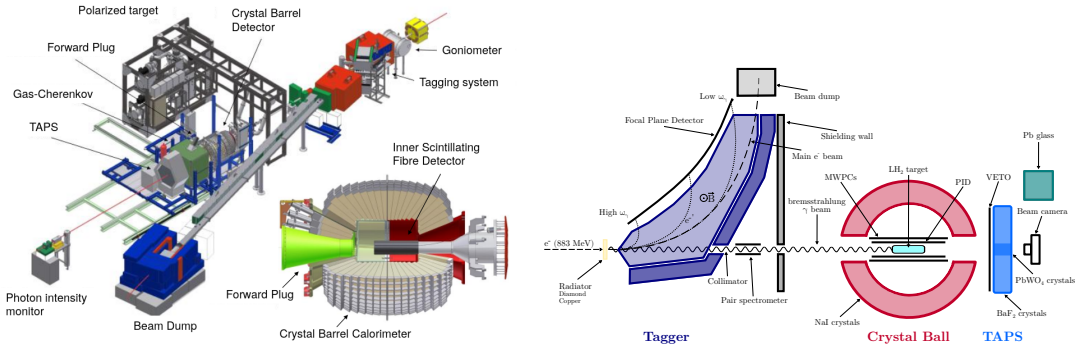

Figure 1: Overview of the CBELSA/TAPS experiment at ELSA (left) [6] and the Crystal Ball experiment at MAMI (right) [8].

ideally suited to study photoproduction of neutral mesons and measure polarization observables. In 2018, the Crystal Barrel readout electronics were upgraded from slow PIN photodiodes to faster avalanche photodiodes [9]. Together with a newly developed online cluster finder, the trigger efficiency for completely neutral final states has been increased significantly at the CBELSA/TAPS experiment.

3. Recent results for the reaction $\gamma p \to p\pi^0$

Fig. 2 shows how much data for the unpolarized cross section as well as for polarization observables has been collected for many different photoproduction reactions since the year 2000 [10]. The $p\pi^0$ final state is by far the best measured final state. In 2015, the A2 collaboration published differential cross sections for the $\gamma p \to \pi^0 p$ reaction up to a center of mass energy of $W = 1.9$ GeV with unprecedented fine energy and angular binning, statistical precision and full angular coverage, thus increasing the existing $\pi^0 p$ database by $\sim 47\%$ [7]. Decomposing the differential cross section using Legendre polynomials, the data revealed sensitivity to high partial-wave amplitudes. This high-precision data set plays currently an important role in ongoing partial-wave and coupled-channel analyses. Apart from the measurements of unpolarized cross sections, both the A2 as well as the CBELSA/TAPS collaborations significantly contributed towards collecting data for all polarization observables from the *beam-target* category using polarized photon beams and polarized targets: Σ, T, P, H, E, G, F [6, 11–17]. One intriguing recent measurement is the simultaneous extraction of the polarization observables E and G from data measured for the first time with elliptically polarized photons [3].

3.1 Simultaneous measurement of the polarization observables E and G with elliptically polarized photons

The polarization observables E and G were measured for the first time with elliptically polarized photons, which exhibit both a linear and circular polarization component, at the Crystal Ball

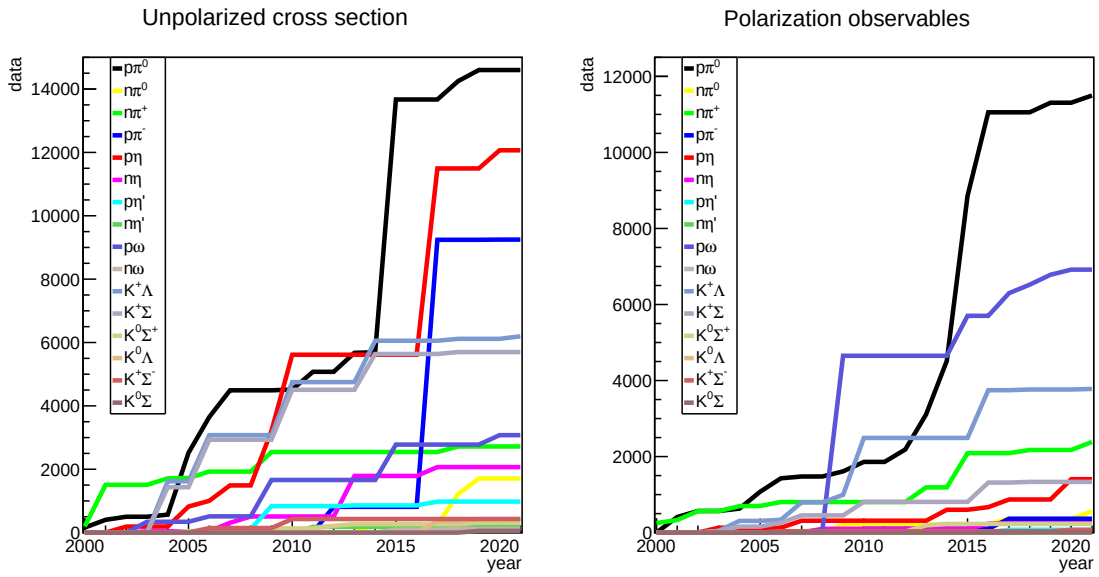

Figure 2: Development of the database in photoproduction of various different final states for the unpolarized cross section (left) and polarization observables (right) since the year 2000 [10].

experiment in the A2 hall at MAMI. This was achieved by using longitudinally polarized electrons in combination with a diamond crystal radiator. The small dependency of the circular polarization degree on the crystal lattice is shown in Fig. 3 top left. Measuring with elliptically polarized photons provides two advantages: the increase in photon flux due to the coherent edge caused by the diamond crystal structure and the possibility to measure several polarization observables simultaneously. The extracted helicity asymmetry E for the $p\pi^0$ and $n\pi^+$ final states is compared to previous CBELSA/TAPS data which were measured with circularly polarized photons using an amorphous radiator (see Fig. 3 top right). Both data sets agree very well with each other within the given uncertainties, emphasizing the applicability of elliptically polarized photons for the measurement of polarization observables.

The measured angular distributions of the helicity asymmetry E multiplied with the differential cross section can be described by a finite series of partial waves which is truncated at a maximal orbital angular momentum $\ell_{\max}$ [18]. While the angular dependence can be described by associated Legendre polynomials, the energy dependence is expressed as a sum of bilinear products of the photoproduction multipoles through the Legendre coefficients. One of these Legendre coefficients, shown in Fig. 3, is sensitive to the interference between S and D partial waves. Here, the $p\eta$ cusp is very clearly visible. A comparison between data and existing model solutions shows that there are discrepancies in how the $p\eta$ cusp is described in their respective approaches.

3.2 $E2/M1$ ratio in the $N \rightarrow \Delta(1232)$ transition

Recently, the A2 collaboration also measured the helicity-dependent differential cross section for the $p\pi^0$ final state for an incoming photon energy range of 150-400 MeV [8]. The main contribution to the electromagnetic transition of $N \rightarrow \Delta(1232)$ is given by the magnetic dipole component $M1$. If there is a d-wave mixture present, the electric quadrupole transition $E2$ would

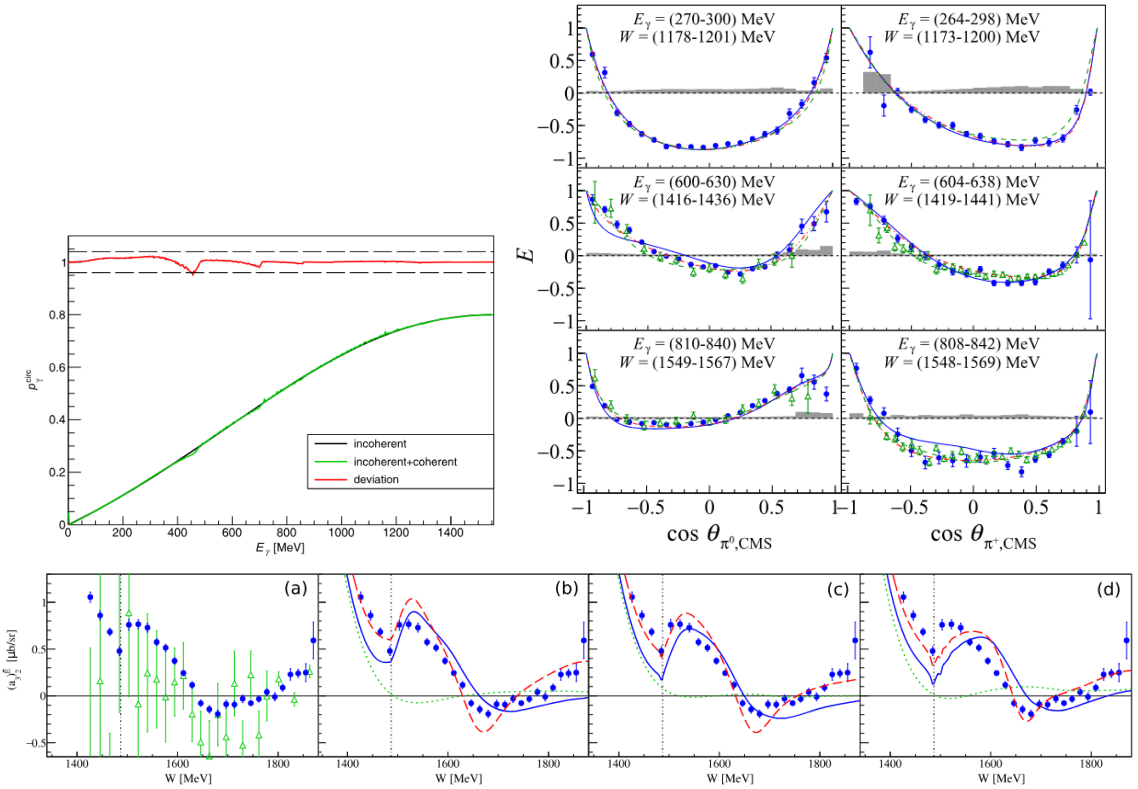

Figure 3: Top left: The calculation of the degree of circular polarization is shown for the case of incoherent bremsstrahlung with an amorphous radiator (black), coherent bremsstrahlung with a diamond radiator (green) and the deviation between the latter two (red). Top right: Comparison of results for the polarization observable E measured with elliptically polarized photons (blue data points) and measured with circularly polarized photons (green data points) for the $p\pi^0$ final state (left column) and the $n\pi^+$ final state (right column). Bottom: The Legendre coefficient $(a_3)_2^E$ (A2 data, blue points) is shown in comparison to (a) CBELSA/TAPS data (green, open triangles) [16], (b) the SAID-MA19, (c) BnGa and (d) JüBo -2017 solutions. [3]

be possible as well. Extracting the ratio $E2/M1$ allows to quantify how much the nucleon and/or $\Delta(1232)$ resonance is different from a spherical shape. To this end, a Legendre moment analysis was performed with the measured angular distributions using a bootstrap-based fitting method and a ratio of $R_{EM} = (-2.38 \pm 0.16 \pm 0.10)$ was determined at the $\Delta(1232)$ mass value. This result is the most precise value reported thus far.

4. Recent results for the reaction $\gamma p \to p\eta$

Over the last years, many high-precision data sets were also measured for the ηp final state by the CBELSA/TAPS and A2 collaborations. A few recent results are highlighted in the following.

4.1 Evidence for the $N(1895)\frac{1}{2}^-$

Apart from the precise measurement of the unpolarized cross section for the $p\pi^0$ final state, the A2 collaboration also measured high-precision cross section data for the $p\eta$ and $p\eta'$ final states

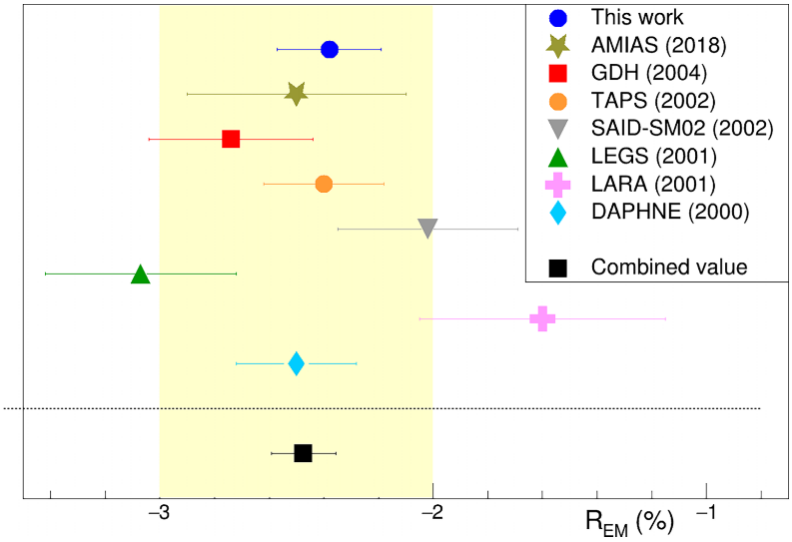

Figure 4: The recently obtained R_{EM} value by the A2 collaboration is shown in comparison to previous values [8].

from their production thresholds up to a center-of-mass energy of $W = 1.96$ GeV with a fine energy binning and full polar angular coverage [19]. The total cross sections are shown in Fig. 5. A strong cusp is visible in the $p\eta$ total cross section at the η' threshold of $W = 1896$ MeV. According to the ηMAID-2018 isobar model [20], the strong observed cusp in the $p\eta$ cross section as well as the fast rise of the $p\eta'$ cross section show a strong coupling to the $N(1895)\frac{1}{2}^-$ to both the $p\eta$ and the $p\eta'$ final states.

Aside from the cross section data also the recently published beam asymmetry Σ data in η

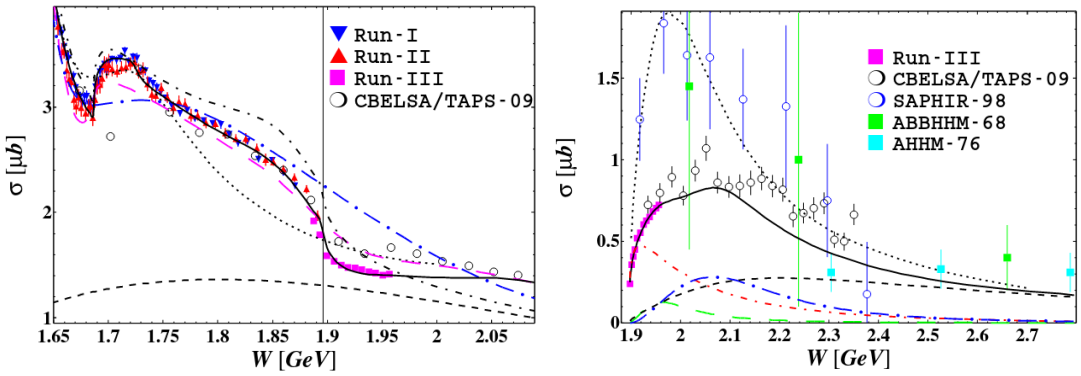

Figure 5: Left: Blue, red and magenta points show the total cross section for the $p\eta$ final state measured by the A2 collaboration. The $p\eta'$ cusp is marked with the vertical line. Right: New A2 data for the total cross section for the $p\eta'$ final state are shown near the photoproduction threshold (magenta points). [19]

photoproduction by the CBELSA/TAPS collaboration shows strong indication for the existence of the $N(1895)\frac{1}{2}^-$ resonance [21]. Fig. 6 shows the beam asymmetry data for different incident photon energies. A backward peak starts to emerge in the angular distributions above the $p\eta'$ threshold ($E_\gamma = 1447$ MeV) which different PWA model solutions did not predict. The backward

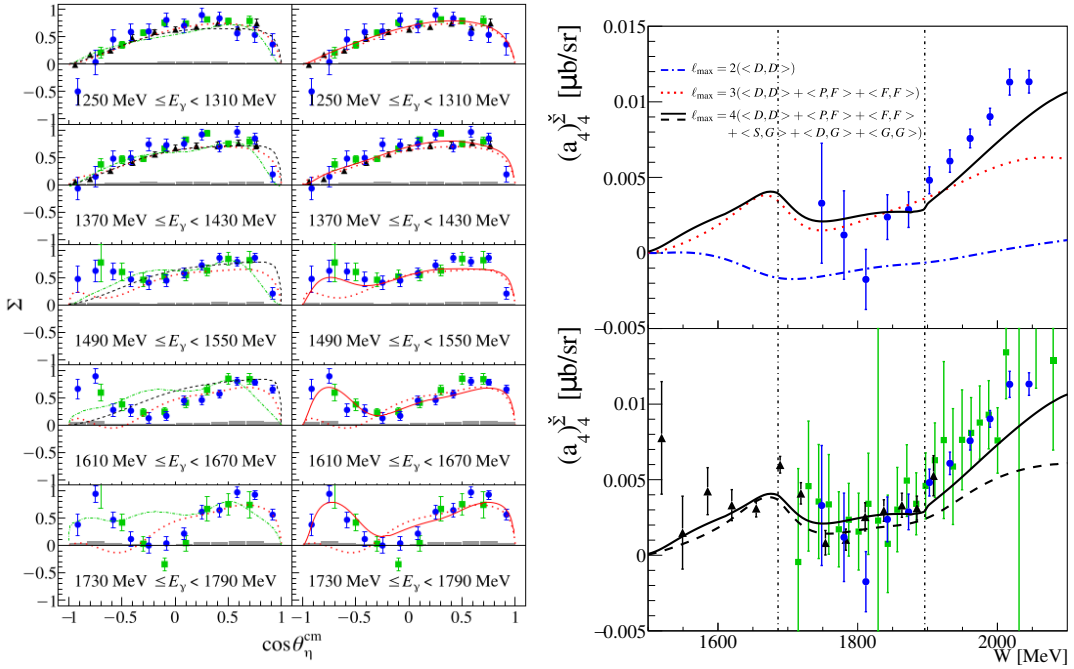

Figure 6: Left: The beam asymmetry Σ in η photoproduction measured by the CBELSA/TAPS experiment. Right: A Legendre coefficient shows the $p\eta'$ cusp. [21]

peak was further investigated using a Legendre moment analysis truncated at $\ell_{max} = 4$ (G waves). The Legendre coefficient $(a_4)_4^\Sigma$, which is sensitive to e.g. the interference between S and G waves, shows a linear rise starting at the η' production threshold. This strongly indicates the presence of a cusp. The inclusion of this beam asymmetry data in a recent BnGa partial wave analysis resulted also in the confirmation of the $N(1895)\frac{1}{2}^-$ resonance and the extraction of its resonance parameters [21]. The $N(1895)\frac{1}{2}^-$ is listed as a four-star resonance in the PDG since 2020 [22].

4.2 $N^* \to p\eta$ branching ratios

The CBELSA/TAPS collaboration reported the measurement of several polarization observables T, E, P, H, and G for the $p\eta$ final state [23]. One example is given by the target asymmetry T in Fig. 7. This new CBELSA/TAPS data together with the above mentioned cross section and beam asymetry data, as well as other data sets from the A2 and CLAS collaborations, a BnGa refit was performed and the branching ratios for $N^* \to N\eta$ were determined. Particularly interesting is the result for the branching ratio $N(1650)\frac{1}{2}^- \to N\eta$ which is reported as 0.33 ± 0.04 [23]. This value is significantly larger than previously reported values and it removes the previously existing discrepancy between the branching ratios of the $N(1535)\frac{1}{2}^-$ and the $N(1650)\frac{1}{2}^-$ resonances which was a topic of much discussion in literature.

5. Measurements off neutrons

In order to determine the isospin decomposition of the reaction amplitudes, it is important to measure data not only off protons, but also off neutrons. In the case of the photoproduction of an

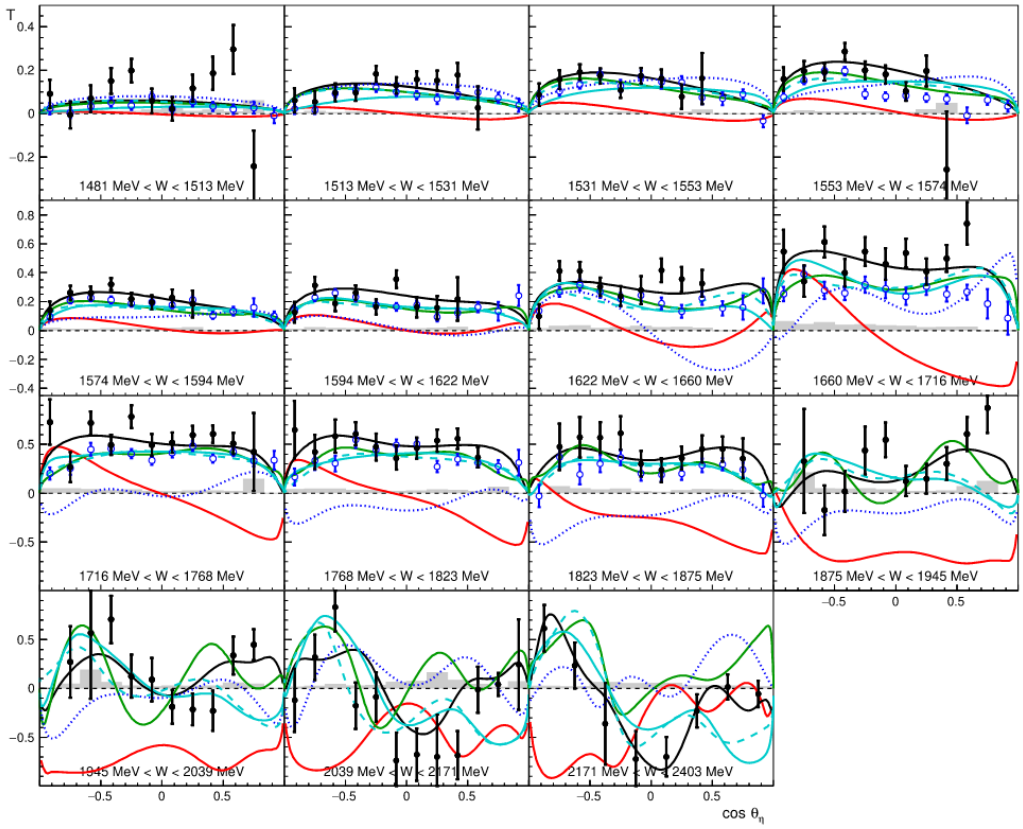

Figure 7: The polarization observable T is shown as a function of $\cos\theta_\eta$ for several center-of-mass energy bins. The data is compared to different model predictions. The BnGa refit including this data is given by the black line. [23]

isoscalar η off protons and off neutrons, the reaction amplitudes are given by a linear combination of the photon isoscalar and an isovector amplitudes A^{IS} and A^{IV}. Since there are no free neutrons available, measurements are performed with quasi-free neutrons bound in e.g. deuteron. Thus, complications due to Fermi motion and final state interaction (FSI) processes occur.

In the ηn final state, a narrow peak was observed at around $W = 1685$ MeV with a width of around 30 MeV. The interpretation of this narrow structure has been much discussed in literature [24]. The most recent models either discuss the narrow peak as an intrinsic resonance or as an interference effect. To shed more light on the origin of this narrow peak, the CBELSA/TAPS collaboration measured the target asymmetry T, recoil asymmetry P, and beam-target double polarization observable H for the first time for the ηn final state (see Fig. 8). A comparison of the new data to different PWA models favors the interpretation of the narrow structure as an interference between the two known S-wave resonances $N(1535)\frac{1}{2}^-$ and $N(1650)\frac{1}{2}^-$.

At present, further analyses for two pseudo-scalar photoproduction off neutrons, like $n\pi^0\pi^0$ and $n\pi^0\eta$, are underway at the CBELSA/TAPS experiment.

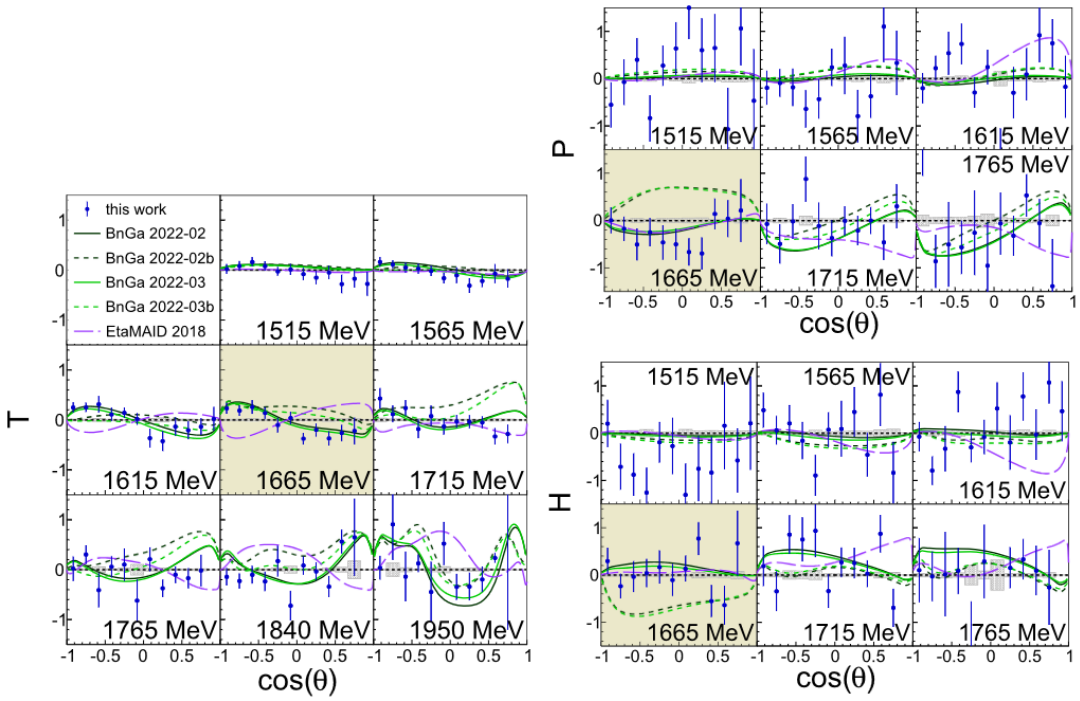

Figure 8: The polarization observables T,P and H are shown for the reaction $\gamma n \to \eta n$ for different center-of-mass energies. The mass range relevant for the observed narrow structure is highlighted in yellow. The curves represent the BnGa 2022-02 (solid black), BnGa 2022-02b (dashed black), BnGa 2022-03 (solid green), BnGa 2022-03b (dashed green curve), EtaMAID-2018 (dashed purple). [24]

6. Summary

Light baryon spectroscopy is an experimentally challenging task. The CBELSA/TAPS at ELSA and the Crystal Ball experiment at MAMI have significantly contributed towards getting a better understanding of the nucleon excitation spectrum. High-precision data sets for the unpolarized cross section as well as many measured polarization observables helped getting sensitivity up to high partial waves, confirm poorly known states like the $N(1895)\frac{1}{2}^-$ and extract branching ratios for different final states.

After decades of studying N^* and Δ^* resonances, a new experiment is planned at ELSA in Bonn called INSIGHT (Investigation of the strong interaction in the light flavor sector) which will focus on studying hyperons.

Acknowledgments

The author is supported by the German Research Foundation (DFG) with the grant number 505387544.

References

[1] U. Loring, B.C. Metsch and H.R. Petry, *The Light baryon spectrum in a relativistic quark model with instanton induced quark forces: The Nonstrange baryon spectrum and ground*

states, *Eur. Phys. J. A* **10** (2001) 395 [hep-ph/0103289].

[2] R.G. Edwards, J.J. Dudek, D.G. Richards and S.J. Wallace, *Excited state baryon spectroscopy from lattice QCD*, *Phys. Rev. D* **84** (2011) 074508 [1104.5152].

[3] A2 collaboration, *First Measurement Using Elliptically Polarized Photons of the Double-Polarization Observable E for $\gamma p \to p\pi^0$ and $\gamma p \to n\pi^+$*, *Phys. Rev. Lett.* **132** (2024) 121902 [2402.05531].

[4] W. Hillert, *The Bonn electron stretcher accelerator ELSA: Past and future*, *Eur. Phys. J. A* **28S1** (2006) 139.

[5] K.H. Kaiser et al., *The 1.5-GeV harmonic double-sided microtron at Mainz University*, *Nucl. Instrum. Meth. A* **593** (2008) 159.

[6] CBELSA/TAPS collaboration, *Measurement of the helicity asymmetry E for the reaction $\gamma p \to \pi^0 p$*, *Eur. Phys. J. A* **57** (2021) 40 [1904.12560].

[7] A2 collaboration, *Measurement of π^0 photoproduction on the proton at MAMI C*, *Phys. Rev. C* **92** (2015) 024617 [1506.08849].

[8] A2 Collaboration at MAMI collaboration, *Evaluation of the $E2/M1$ ratio in the $N \to \Delta(1232)$ transition from the $\vec{\gamma}\vec{p} \to p\pi^0$ reaction*, *Phys. Rev. C* **109** (2024) 055201 [2312.08211].

[9] CBELSA/TAPS collaboration, *The new APD-Based Readout of the Crystal Barrel Calorimeter – An Overview*, 2212.12364.

[10] A. Thiel, F. Afzal and Y. Wunderlich, *Light Baryon Spectroscopy*, *Prog. Part. Nucl. Phys.* **125** (2022) 103949 [2202.05055].

[11] CBELSA/TAPS collaboration, *Double-polarization observable G in neutral-pion photoproduction off the proton*, *Eur. Phys. J. A* **53** (2017) 8 [1604.02922].

[12] MAINZ-A2 collaboration, *Photon asymmetry measurements of $\vec{\gamma}p \to \pi^0 p$ for E_γ = 320-650 MeV*, *Eur. Phys. J. A* **52** (2016) 333 [1606.07930].

[13] A2, MAMI collaboration, *T and F asymmetries in π^0 photoproduction on the proton*, *Phys. Rev. C* **93** (2016) 055209.

[14] CBELSA/TAPS collaboration, *The polarization observables T , P , and H and their impact on $\gamma p \to p\pi^0$ multipoles*, *Phys. Lett. B* **748** (2015) 212 [1506.06226].

[15] J. Hartmann et al., *The N(1520) 3/2- helicity amplitudes from an energy-independent multipole analysis based on new polarization data on photoproduction of neutral pions*, *Phys. Rev. Lett.* **113** (2014) 062001 [1407.2163].

[16] CBELSA/TAPS collaboration, *First measurement of the helicity asymmetry for $\gamma p \to p\pi^0$ in the resonance region*, *Phys. Rev. Lett.* **112** (2014) 012003 [1312.2187].

[17] A2, CB-TAPS collaboration, *Accurate Test of Chiral Dynamics in the $\gamma p \to \pi^0 p$ Reaction*, *Phys. Rev. Lett.* **111** (2013) 062004 [1211.5495].

[18] Y. Wunderlich, F. Afzal, A. Thiel and R. Beck, *Determining the dominant partial wave contributions from angular distributions of single- and double-polarization observables in pseudoscalar meson photoproduction*, *Eur. Phys. J. A* **53** (2017) 86 [1611.01031].

[19] A2 collaboration, *Study of η and η' Photoproduction at MAMI*, *Phys. Rev. Lett.* **118** (2017) 212001 [1701.04809].

[20] L. Tiator, M. Gorchtein, V.L. Kashevarov, K. Nikonov, M. Ostrick, M. Hadžimehmedović et al., *Eta and Etaprime Photoproduction on the Nucleon with the Isobar Model EtaMAID2018*, *Eur. Phys. J. A* **54** (2018) 210 [1807.04525].

[21] CBELSA/TAPS collaboration, *Observation of the $p\eta$' Cusp in the New Precise Beam Asymmetry Σ Data for $\gamma p \to p\eta$*, *Phys. Rev. Lett.* **125** (2020) 152002 [2009.06248].

[22] P.D. Group, P.A. Zyla, R.M. Barnett, J. Beringer, O. Dahl, D.A. Dwyer et al., *Review of particle physics*, *Progress of Theoretical and Experimental Physics* **2020** (2020) 083C01 [https://academic.oup.com/ptep/article-pdf/2020/8/083C01/34673722/ptaa104.pdf].

[23] CBELSA/TAPS collaboration, *New data on $\vec{\gamma}\vec{p} \to \eta p$ with polarized photons and protons and their implications for $N^* \to N\eta$ decays*, *Phys. Lett. B* **803** (2020) 135323 [1909.08464].

[24] CBELSA/TAPS collaboration, *Measurement of polarization observables $\boldsymbol{T}$, $\boldsymbol{P}$, and $\boldsymbol{H}$ in π^0 and η photoproduction off quasi-free nucleons*, *Eur. Phys. J. A* **59** (2023) 232.